JOC The Journal of Organic Chemistry

pubs.acs.org/joc Article

Development of Aromatic Foldamer Building Blocks Bearing Multiple Biogenic Side Chains

Márton Zwillinger,[#] Petra Sőregi,[#] Florian Sanchez,[#] Céline Douat, Márton Csékei, Ivan Huc,* and András Kotschy*

Cite This: J. Org. Chem. 2025, 90, 3043−3052 Read Online

ACCESS | Metrics & More | Article Recommendations | Supporting Information

ABSTRACT: Aromatic oligoamides, with their intrinsic rigidity and well-defined conformations, are recognized for their potential in medical applications. Similar structures are present in several naturally occurring antibiotics and have been explored for their ability to bind to various proteins and B-DNA (canonical right-handed DNA helix). This study introduces a synthetic approach to produce quinoline amino acid monomers bearing diversified side chain combinations in positions 4, 5, and 6 of the quinoline ring, designed to enhance the side chain density on helical foldamers. By increasing the number of side chains on each monomer, we aim to mimic the dense side chain presentation of α-peptides, thus improving the potential for protein surface recognition. This synthetic strategy involves efficient functionalization through cross-coupling reactions, enabling the installation of diverse side chains at strategic positions on the quinoline ring. The process has been optimized for automated solid-phase synthesis, successfully producing a 20-unit oligoamide with good purity. This foldamer, featuring multiple cationic, anionic, polar, and hydrophobic side chains, demonstrates the potential for molecular recognition in drug discovery and therapeutic applications. The methodology described here represents a significant advancement in the construction of aromatic oligoamide foldamers, providing a robust platform for further exploration of biological systems.

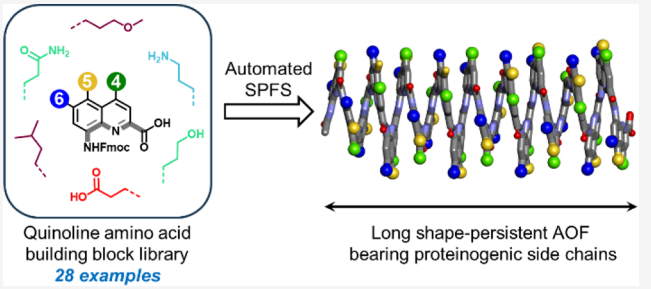

INTRODUCTION

Thanks to their intrinsic rigidity and well-defined conformations, aromatic oligoamides are considered privileged structures for medical applications.[1−8] Several naturally occurring antibiotics contain aromatic amide units, including cystobactamids[9] and albicidin,[10,11] as well as distamycin A and its analogues, netropsin and anthelvencin C.[12−14] The latter family has been the object of considerable development toward sequence-specific oligo-pyrrole-imidazole minor groove binders of B-DNA.[15,16] Along the same line, the old arylamide antiparasitic drug suramin has been shown to bind to a large number of proteins[5−8] and the design of suramin analogs is the object of current investigations.[17−19]

In parallel, along with other rigid backbones,[20−26] aromatic oligoamide foldamers have been developed as scaffolds to display proteinogenic side chains at defined positions in space. These may be divided into short rod-like oligomers with amphipathic structures that may have antibiotic activity,[27,28] rod-like oligomers that mimic α-helices,[29−35] and helically folded oligoarylamides that may cover large surface areas of proteins,[36−38] interfere with amyloid aggregation,[39,40] or mimic the B-DNA structure and competitively inhibit DNA−protein interactions.[41−44]

The field of aromatic oligoamide foldamers is driven by the continuous development of new monomers, and particularly by the availability of a variety of side chains that can be tethered at various positions of the aromatic units (Figure 1). In the case of 8-amino-2-quinoline carboxylic acid (Figure 1), one of the most frequently employed δ-amino acid building blocks of the helically folded oligoarylamides mentioned above, efforts have already been made toward producing main chain variations using pyridine- or benzene-based monomers,[45] and to control helix handedness.[46−50] Methods to install various proteinogenic side chains in positions 4, 5, or 6 of the quinoline ring are also available.[51,52] However, such δ-amino acid monomers may be considered as equivalents to dipeptides, and a dipeptide possesses two side chains. It follows that helices of 8-amino-2-quinoline carboxylic acid-derived oligoamides bearing only one side chain per monomer have a relatively scattered side chain presentation at their surface and largely expose their main chain to the solvent, thus reducing opportunities for interactions with biological targets. Installing additional side chains on each monomer would instead enable a high side chain density at the

Received: November 25, 2024
Revised: January 21, 2025
Accepted: January 30, 2025
Published: February 18, 2025

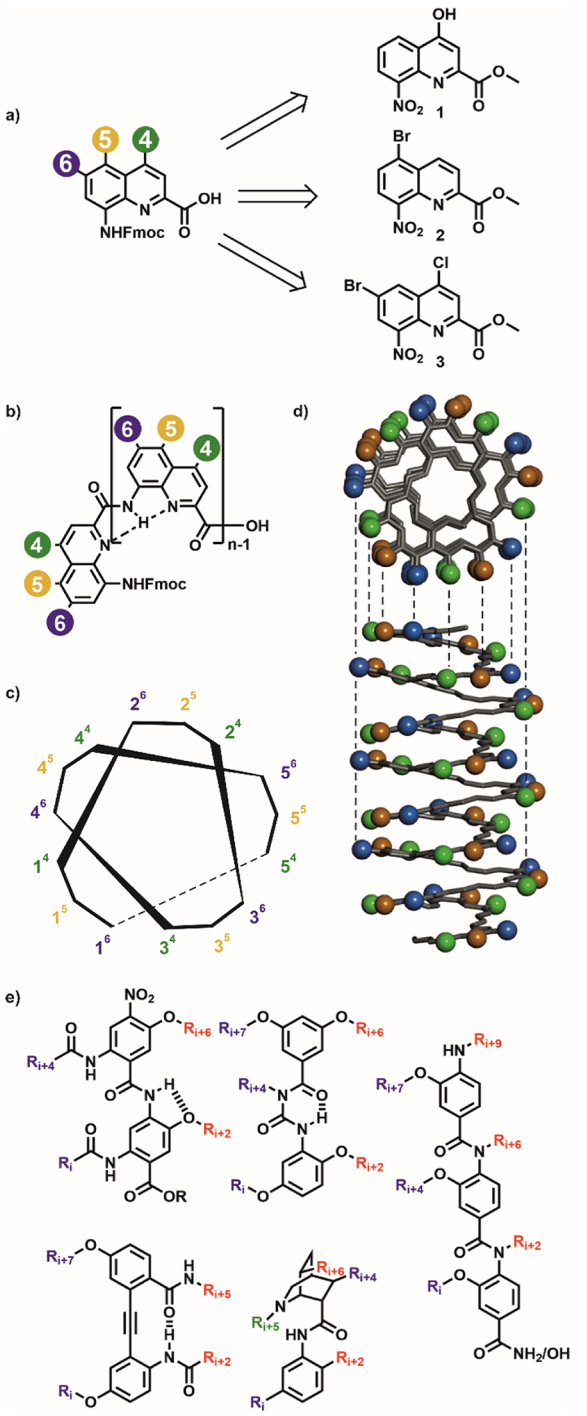

Figure 1. (a) Representation of the different precursors for the synthesis of monomer building blocks bearing side chains in positions 4 (green), 5 (gold), and 6 (blue). (b) Chain elongation of an aromatic oligoamide foldamer. Hydrogen bonds on the inner rim of the helix are indicated as dashed lines. (c) Schematic representations of an 8-amino-2-quinolinecarboxylic acid oligoamide helix showing the density of side chains in position 4 (green), 5 (gold), and 6 (blue). Numbers indicate monomer unit position in the sequence, while superscript numbers indicate side chain position on a given quinoline monomer. (d) Top view and side view of a molecular model of an aromatic oligoamide foldamer showing the substitution position in 4 (green spheres), 5 (gold spheres), and 6 (blue spheres). (e) Examples of multifacial α-helix mimetics having two side chains per monomer taken from ref 31. The side chain numbers correspond to equivalent residue positions in an α-helical α-peptide sequence.

surface of such helices (Figure 1). The issue of low side chain density has already been addressed for rod-like oligoamides, leading to the design and synthesis of multifacial α-helix mimetics bearing two side chains per monomer (Figure 1d).[31,53,54]

Here, we describe an efficient synthetic approach to produce 4,6-disubstituted 8-amino-2-quinoline carboxylic acid monomers. We also expand the diversity of monomers bearing a single side chain at positions 4, 5 or 6. Combined with previously described monomers,[41,42,51,52] the new monomers offer innumerable combinations for side chain presentation on helically folded oligoarylamides.

RESULTS AND DISCUSSION

General Concept. It has been illustrated that a single face of an aromatic foldamer helix, constructed using 4- and 6-substituted quinoline building blocks, can effectively project side chains at positions mimicking those of a polypeptide's α-helix.[51] A crucial aspect in achieving this lies in the increased density of side chains, which create a potential binding motif on one face of the foldamer helix. While relocating specific side chains by altering the substitution pattern of a few monomers within a sequence can result in a localized increase in side chain density, a broader adjustment would be achieved by raising the number of residues carried by the same backbone. We surmised that doubling the number of side chains carried by each quinoline unit would result in a side chain density resembling that observed in α-peptides and proteins. The surface of helices with increased side chain density would be richer in information and better suited for protein surface recognition (Figure 1).

To enable the creation of helical foldamers with modified surface substitution patterns, we designed an array of novel quinoline-based monomers. The designed building blocks feature suitably protected cationic, anionic, polar neutral, and hydrophobic side chains attached to positions 4, 5, or 6 of the quinoline, respectively. To introduce side chains at these positions, three previously described, easily accessible quinoline derivatives were used as starting materials: methyl-4-hydroxy-8-nitro-quinoline-2-carboxylate (**1**),[55] methyl-5-bromo-8-nitro-quinoline-2-carboxylate (**2**)[52] and methyl-6-bromo-4-chloro-8-nitro-quinoline-2-carboxylate (**3**).[51] The 4-hydroxy group of **1** can be utilized in nucleophilic substitutions to yield monomers with oxygen-linked side chains. It can also be converted to a 4-chloro or 4-bromo group. Chloro or bromo substituents in position 4, 5, or 6 can be engaged in carbon−carbon cross-coupling reactions. Efficient functionalization was achieved by sp^2-sp^3 (Suzuki), sp^2-sp^2 (Suzuki, Heck), or sp^2-sp (Sonogashira) cross-couplings. The choice of method depended on the nature of the side chain and the availability of its precursor. Notably, side chain synthons could be either alkynes, alkenes, or alkenyl- or alkyl-boron reagents, thus offering a broad spectrum of potential precursors. Compound **3** possesses both a 4-chloro and a 6-bromo substituent, which can be involved in cross-coupling reactions sequentially, giving access to 4,6-difunctionalized monomers. Finally, the monomers were all delivered in a protected form, ready for solid-phase foldamer synthesis,[56] that is, with a free carboxylic acid in position 2, a Fmoc-protected amine in position 8, and suitable acid-labile protecting groups on their side chains. We discuss below the different routes and the synthetic hurdles with which we had to cope.

Preparation of 4-Monosubstituted Quinoline Derivatives. Several 4-monosubstituted monomers have been

https://doi.org/10.1021/acs.joc.4c02900
J. Org. Chem. 2025, 90, 3043−3052

designed and synthesized, utilizing key intermediates **1** and **4** as starting materials (Scheme 1). The diversity of the new side

Scheme 1. Synthetic Pathway of 4-Monosubstituted *N*-Fmoc Quinoline Monomers 7a−d[a]

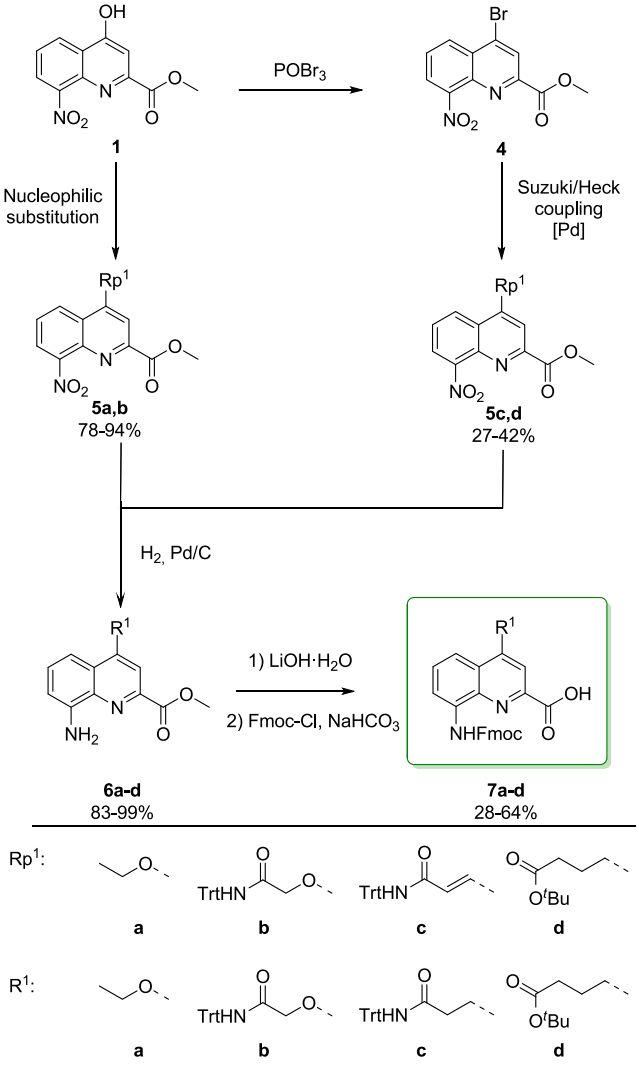

[a]$Pd(OAc)_2$ and tris(*o*-tolyl)phosphine $P(oTol)_3$ were used to obtain intermediate **5c**. Intermediate **5d** was synthesized using bis(di-*tert*-butyl(4-dimethylaminophenyl)phosphine)dichloropalladium(II) Pd-$(AtaPhos)_2Cl_2$.

chains is not extensive, as they simply complement a broad range of hydrophobic, anionic, cationic, and polar neutral side chains already introduced in position 4.[41,42,51,52] Side chains with primary amide functions were desirable as asparagine and glutamine analogues. The synthon **1** has been previously used to prepare a variety of quinoline-based monomers, where the hydroxyl group in position 4 could participate in nucleophilic substitution reactions, leading to aryl-alkyl ether linkages.[52] As depicted in Scheme 1, the nucleophilic substitution of ethyl iodide with **1** furnished intermediate **5a** in good yield, and then the nitro group was reduced by catalytic hydrogenation to give **6a** in quantitative yield. For the preparation of intermediate **5b**, the primary amide was protected with a trityl group.[57] The nucleophilic substitution of 2-bromo-*N*-tritylacetamide with **1** proceeded smoothly, and **6b** was isolated in good yield after subsequent catalytic hydrogenation of **5b** (Scheme 1).

The 4-bromo group of precursor **4**[31] served as the aryl halide in cross-coupling reactions. For the introduction of *N*-tritylpropionamide (**5c**) and *tert*-butyl-butyrate (**5d**) side chains, a Heck coupling of the corresponding alkene derivative with **4**, followed by saturation of the double bond, was envisaged. In the case of the *N*-trityl-protected acrylamide, Heck coupling furnished intermediate **5c** in moderate yield (42%), which was then hydrogenated to give **6c** in 83% yield. In contrast, attempts to perform Heck coupling with *tert*-butyl-but-3-enoate failed. An alternative approach could have been to perform a Sonogashira coupling in the presence of *tert*-butyl-but-3-ynoate, but purchasing or synthesizing this reactant was not practical. A third approach consisted of using boron derivatives in Suzuki coupling.

Since the appropriate alkenyl boronate derivative was not available, we generated the alkyl analog *in situ* from the alkene and 9-BBN.[51] Indeed, the hydroboration of *tert*-butyl-but-3-enoate with 9-BBN gave the corresponding trialkylborane precursor, which was successfully used in the following sp^2-sp^3 Suzuki coupling to give **5d** in a moderate yield (27%). Subsequent hydrogenation of the nitro group yielded **6d** with a good yield (87%). Earlier, we reported a one-pot method to convert amino esters to *N*-Fmoc protected amino acids.[51] Starting from **6a−d**, this method gave monomers **7a−d** in moderate to good yields.

Preparation of 5-Monosubstituted Quinoline Monomers. In a second stage, five new 5-monosubstituted monomers were designed, carrying cationic and aliphatic side chains in position 5 (Scheme 2). Again, these side chains are additions to

Scheme 2. Synthetic Pathway of 5-Monosubstituted *N*-Fmoc Quinoline Monomers 10a−e[a]

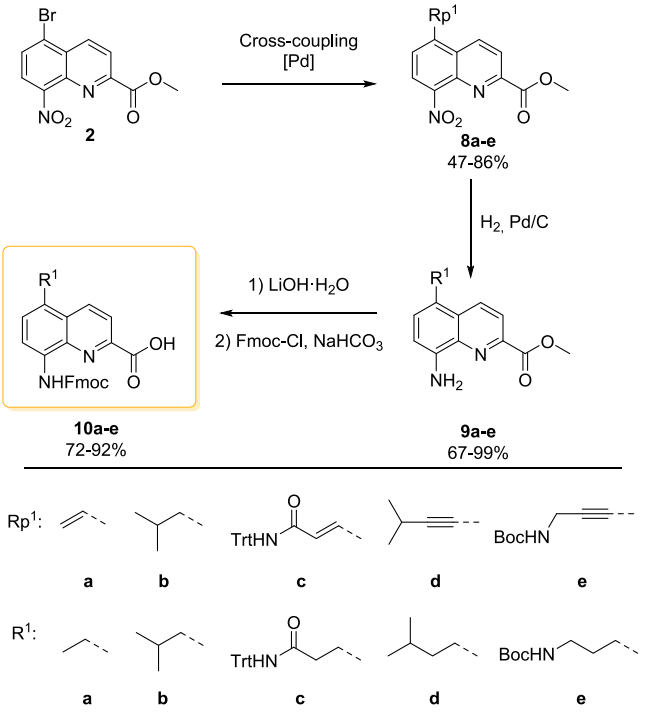

[a]Cross-couplings involved the use of $Pd(OAc)_2$ and SPhos (Dicyclohexyl(2′,6′-dimethoxy[1,1′-biphenyl]-2-yl)phosphine) or P-$(oTol)_3$ for intermediates **8a** and **8c**, respectively. $Pd(PPh_3)_2Cl_2$ was used for the synthesis of intermediates **8b**, **8d**, and **8e**. $P(oTol)_3$ was added for intermediate **8e**.

https://doi.org/10.1021/acs.joc.4c02900
J. Org. Chem. 2025, 90, 3043−3052

an existing series. For example, several anionic side chains containing a carboxylic or phosphonic acid function have been previously introduced in position 5.[41,42,52] Their common starting material was the 5-bromoquinoline derivative **2**, which was converted into intermediates **8a−e** by using various cross-coupling reactions. Hence, **8a** and **8b** were prepared via Suzuki couplings, where potassium vinyltrifluoroborate and isobutylboronic acid were used as side chain synthons, respectively. For the introduction of the *N*-trityl-propionamide side chain, *N*-trityl-acrylamide was employed in a Heck coupling reaction to produce **8c**. Compounds **8d** and **8e** were synthesized via Sonogashira reactions using the appropriate alkynes. Subsequently, all five amino esters **9a−e** were isolated in good to quantitative yields after a catalytic hydrogenation reaction, where both the nitro group and the unsaturated carbon−carbon bonds were reduced. Further hydrolysis of the amino esters and *N*-Fmoc protection of the newly obtained amino acids were performed to obtain the final **10a−e** monomers in good yields.

Selective Functionalization at Position 6 to Furnish 6-Monosubstituted Quinoline Monomers. In a previous work, we reported a robust synthesis allowing the efficient installation of various side chains in position 6 and the production of *N*-Fmoc-protected-6-substituted aminoquinoline carboxylic acid monomers on a gram scale.[51] The approach is based on selective cross-coupling at the 6-position of methyl 6-bromo-4-chloro-8-nitro-2-quinolinecarboxylate (**3**). By adapting this methodology, five new 6-monosubstituted quinoline monomers were prepared, allowing us to broaden the repertoire of side chains available at this position of the quinoline ring (Scheme 3). To introduce the *iso*pentyl and *n*-butyl side chains, we opted for the alkyne synthons 3-methyl-but-1-yne and but-1-yn-1-yltrimethylsilane, respectively. The latter could be easily deprotected *in situ* by using H_2SiF_6. The Sonogashira coupling of these two synthons proceeded smoothly, and the reaction took place regioselectively on the bromine to furnish **11a** and **11b** in good yields, leaving the chlorine untouched. The alkynyl synthons needed for the introduction of isopropyl and isobutyl side chains do not exist, so we started from the appropriate alkenyl boronates, whose Suzuki coupling yielded the desired derivatives **11c** and **11d**. This time, the regioselectivity was poor, and significant amounts of the 4,6-disubstituted products were also obtained in both cases. To introduce a propionate side chain, we attempted to perform the Sonogashira reaction of **3** with *tert*-butyl propiolate, but it failed under several conditions. To overcome this difficulty, we used *tert*-butyl acrylate in Heck coupling. This transformation was selective, and **11e** was isolated in acceptable yield. Intermediates **11a−e** were further transformed by hydrogenation, which allowed the simultaneous (i) dechlorination in position 4, (ii) saturation of the side chains, and (iii) reduction of the nitro group to produce the corresponding amino esters **12a−e** in moderate to good yields. Subsequent hydrolysis and *N*-Fmoc protection were carried out, yielding the *N*-Fmoc-protected-6-substituted amino-quinoline carboxylic acid monomers **13a−e** in fair to good yields.

Scheme 3. Synthetic Pathway of 6-Monosubstituted *N*-Fmoc Quinoline Monomers 13a−11e[a]

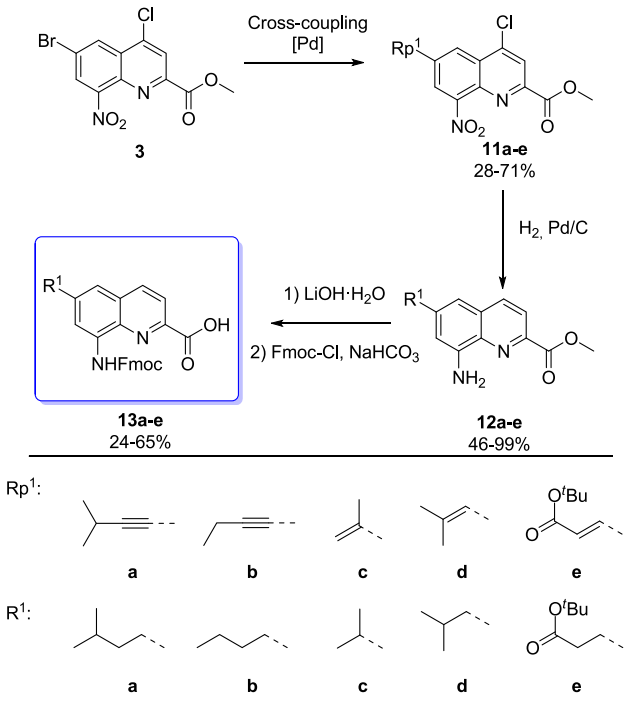

[a]Cross couplings involved different palladium-based catalysts: Pd(PPh$_3$)$_2$Cl$_2$ (**11a−b**), [1,1′-Bis(diphenylphosphino)ferrocene]-palladium(II) dichloride, Pd(dppf)Cl$_2$ (11c and 11d), and Pd(PPh$_3$)$_4$ with P(^{t}Bu)$_3$ (**11e**).

Sequential Side Chain Introduction to Furnish 4,6-Disubstituted Monomers. For 4,6-disubstituted monomers, we wished to install a broad spectrum of side chain characteristics, including hydrophobic, polar neutral, cationic, and anionic moieties, and selected 10 combinations to construct a mini library. Of course, possible combinations are endless. Starting from **3**, functionalization in position 6 afforded **11a** as presented above, as well as previously described **14a** and **14b** (Scheme 4a).[51] The functionalization at position 4 of these compounds was attempted using commercial alkene precursors that were converted to alkylboranes in the presence of 9-BBN to perform sp^2-sp^3 Suzuki couplings. However, these couplings failed, which we attributed to the nitro group that caused undesired side reactions. To circumvent this problem, reduction was brought forward in the synthetic sequence, preceding the cross-coupling. The simultaneous reduction of the side chain triple bond and the 8-nitro group was achieved using mild catalytic hydrogenation over Raney nickel at room temperature, while the chlorine in position 4 remained untouched, yielding **15a−c**. Subsequent two-step, one-pot hydroboration and Suzuki coupling reactions successfully gave access to intermediates **16a−e** in moderate to good yields. The temperature and reaction time for hydroboration and coupling reactions were adjusted for each alkene precursor, as their electronic properties significantly influenced both reactions. Electron-rich alkenes underwent rapid and clean hydroboration, whereas *tert*-butyl acrylate exhibited slower reactivity and produced byproducts. We have also assessed Heck or Sonogashira reactions as potential alternatives, but the Suzuki couplings demonstrated superior performance.

Two other 6-substituted 4-chloroquinolines, **19a** and **19b**, were prepared via regioselective Suzuki coupling from readily available intermediate **18**[51] in moderate to good yields (Scheme 4b). In the subsequent step, **19a** and **19b** were coupled with a second set of alkylboranes to yield *N*-trifluoroacetylated amino esters **20a−e** bearing two different side chains. The one-pot hydrolysis of the amide and ester functions and *N*-Fmoc installation were carried out similarly on intermediates **16a−e** and **20a−e** to obtain the final 4,6-disubstitued monomers **17a−e** and **21a−e** in moderate to good yields.

https://doi.org/10.1021/acs.joc.4c02900
J. Org. Chem. 2025, 90, 3043−3052

Scheme 4. Synthetic Pathways of 4,6-Disubstituted *N*-Fmoc Quinoline Monomers Bearing Different Side Chains[a]

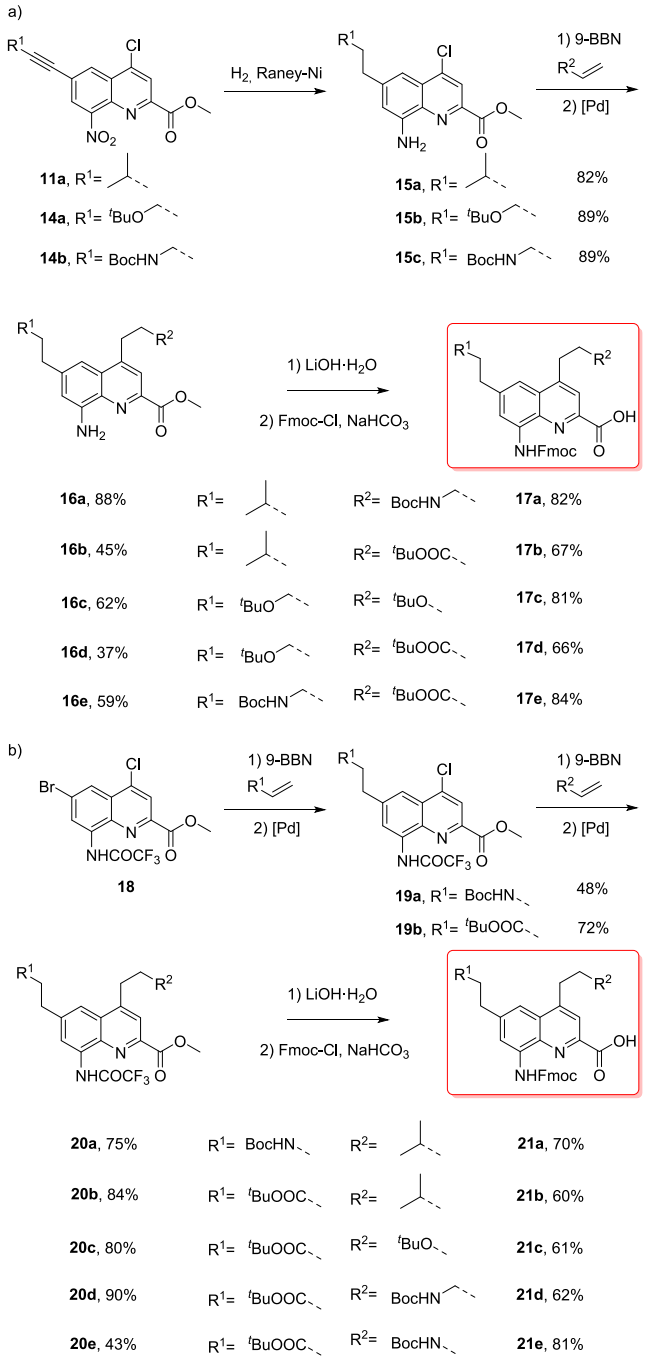

[a]Intermediates **16a−d**, **19b**, and **20a−e** were obtained using $Pd(AtaPhos)_2Cl_2$. Tris(dibenzylideneacetone)dipalladium(0) $Pd(dba)_3$ and diethyl(4-dimethylaminophenyl)phosphine were used for intermediate **16e**.

Concomitant Introduction of the Same Side Chain in Positions 4 and 6 of Quinoline Monomers. The presence of the halogen atoms in both the 4- and 6-positions allows for the incorporation of the same side chain at the same time. Coupling of intermediate **18** with the alkylborane derived from *tert*-butylvinyl ether led to the simultaneous production of the monosubstituted product **22a** (which relates to **19a** and **19b**) and the disubstituted product **22b** in 66% and 25% yields, respectively (Scheme 5a). Intermediate **23** was further hydrolyzed to obtain the amino acid, which, after *N*-Fmoc protection, gave monomer **28d** in 50% yield. While the lower reactivity of chlorine at position 4 is advantageous for regioselective couplings, it is disadvantageous when the same side chain is introduced in both positions, as reflected by the low yield of **22b**. To enhance the reactivity at position 4, the 4,6-dibromo quinoline derivative **23** was synthesized from the 6-bromo-4-hydroxy precursor using $POBr_3$.[58] Double Sonogashira couplings gave access to the desired bisalkyne-functionalized quinoline intermediates **24a** and **24b** in good yield (Scheme 5b).

In the case of the propionate side chain, Heck coupling showed significant dehalogenation. When the nitro group of intermediate **23** was carefully reduced over Raney nickel to the amine **25**, the Heck coupling with *tert*-butyl acrylate proceeded smoothly, and intermediate **26** was isolated in 74% yield. Subsequent saturation of the double and triple bonds of **24a−b** and **26** by catalytic hydrogenation gave **27a−c** in a good yield. The one-pot hydrolysis of the obtained amino esters to amino acids, followed by the *N*-Fmoc protection of the 8-amino group, afforded the foldamer building blocks **28a−c** with fair to good yields.

The complete list of the synthesized monomers and the cumulative yields of their synthesis are listed in the Supporting Information Section 3.5. It is difficult to observe any relationship between the efficiency of the synthesis and the nature of the side chain, which is probably not surprising if we consider the fact that all polar side chains are present in a protected form, which masks their differences in character.

Automated Foldamer Synthesis. The development of efficient peptide screening methods in drug discovery, such as display selection, has renewed interest in peptides in both academic and industrial research. Simultaneously, advancements in the automation of peptide synthesis, as well as the release of new synthesizers, have made solid-phase peptide synthesis accessible to many laboratories.[59] In this context, we have developed effective and reliable methods to synthesize helical aromatic oligoamide foldamers on solid phase, and we have recently automated the process.[56] We sought to challenge our automated solid-phase synthesis protocol using the collection of new monomers and set out to build a 20-unit-long, ∼5.3 kDa large sequence comprised of 20 different monomers. For laboratories not equipped with a suitable automated synthesizer, the manual solid-phase synthesis of a 20mer is perfectly doable using microwave heating and *in situ* acid chloride activation protocols adapted from the Appel reaction.[60,61] In contrast, the solution-phase synthesis of such a molecule would be extremely tedious, even to an experienced chemist. To demonstrate the usefulness of the monomers as well as the power of the synthesizer, we selected the 20 building blocks to exhibit multiple cationic, anionic, polar, or hydrophobic moieties on the different faces of the helix and designed foldamer **29** (see Figure 2d). This target foldamer would be comparable to an α-peptide containing each of the 20 natural amino acids in terms of synthetic effort, albeit being twice as large and bearing more than 20 side chains. Note that **29** is achiral and should thus exist as a racemic mixture of right- and left-handed helical conformers. If a one-handed helix is desired, for example, to target a protein diastereoselectively, absolute handedness control can be achieved by introducing chiral residues.[46−50] Alternatively, protein-foldamer interactions may also bias helix handedness of an otherwise achiral foldamer.[37,38,62]

https://doi.org/10.1021/acs.joc.4c02900
J. Org. Chem. 2025, 90, 3043−3052

Scheme 5. Synthetic Pathways of 4,6-Disubstituted *N*-Fmoc Quinoline Monomers Bearing the Same Side Chain[a]

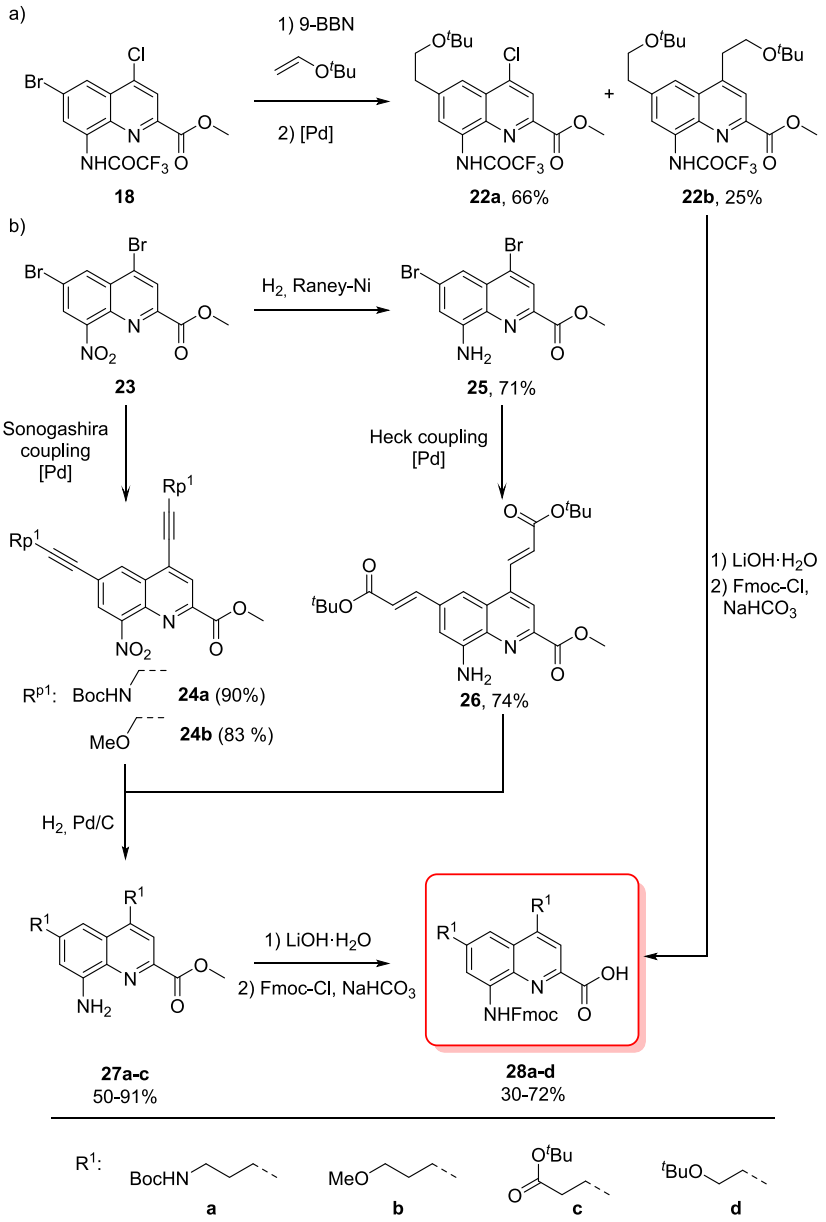

[a]Intermediates **22b** and **24a−b** were obtained using $Pd(AtaPhos)_2Cl_2$. $Pd(OAc)_2$ and $P(oTol)_3$ were used for the intermediate **26.**

The 4,6-disubstituted monomer **28c** was preloaded on a Tentagel Wang resin (low loading, 15 μmol scale), which allows for better bead swelling and gives cleaner crude profiles for long sequences.[63] The subsequent coupling of 19 different Fmoc-protected quinoline monomers was performed on the automated synthesizer, applying deprotection and coupling conditions as depicted in Figure 2a. Of note, recent optimization of the reaction conditions[64] showed that the Fmoc deprotection using 2% DBU in NMP could be shortened to two times 3 min (previously 2 × 10 min) with no measurable loss of efficiency. Coupling conditions involved, as before, the *in situ* acid chloride formation in the preactivation vessel by relying on the Appel reaction with PPh_3 and trichloroacetonitrile (TCAN), before transferring the solution to the reaction vessel containing the resin swollen in anhydrous THF and 2,4,6-collidine. Couplings were performed twice at 50 °C for 15 min. With that, a coupling/deprotection cycle lasts less than an hour, and the whole 20mer (**29**) could be produced in around 15 h. After final acetylation of the resin-bound 20mer, side chain deprotection and cleavage from the resin were performed in a TFA solution containing 2.5% TIPS and 2.5% water as scavengers.

The reverse-phase HPLC (RP-HPLC) analysis of the recovered crude foldamer was encouraging, showing 55% purity. A second peak with a relatively high intensity was also visible on the chromatogram (marked with a red star in Figure 2b), but we were unable to identify this impurity by mass spectrometry. The 20mer **29** was purified by semi-preparative RP-HPLC, and its final chromatogram confirmed a purity over 95%. The recovered yield after purification was 10%, which is satisfactory when compared to the isolation of an HPLC-purified peptide of comparable size (i.e., 40 residues). The ^{1}H NMR spectrum recorded in DMF-d_7 showed one set of signals spread over a wide range of chemical shifts characteristic of the quinoline carboxamide helices (Figure 2c). Typical indications of helical

https://doi.org/10.1021/acs.joc.4c02900
J. Org. Chem. 2025, 90, 3043−3052

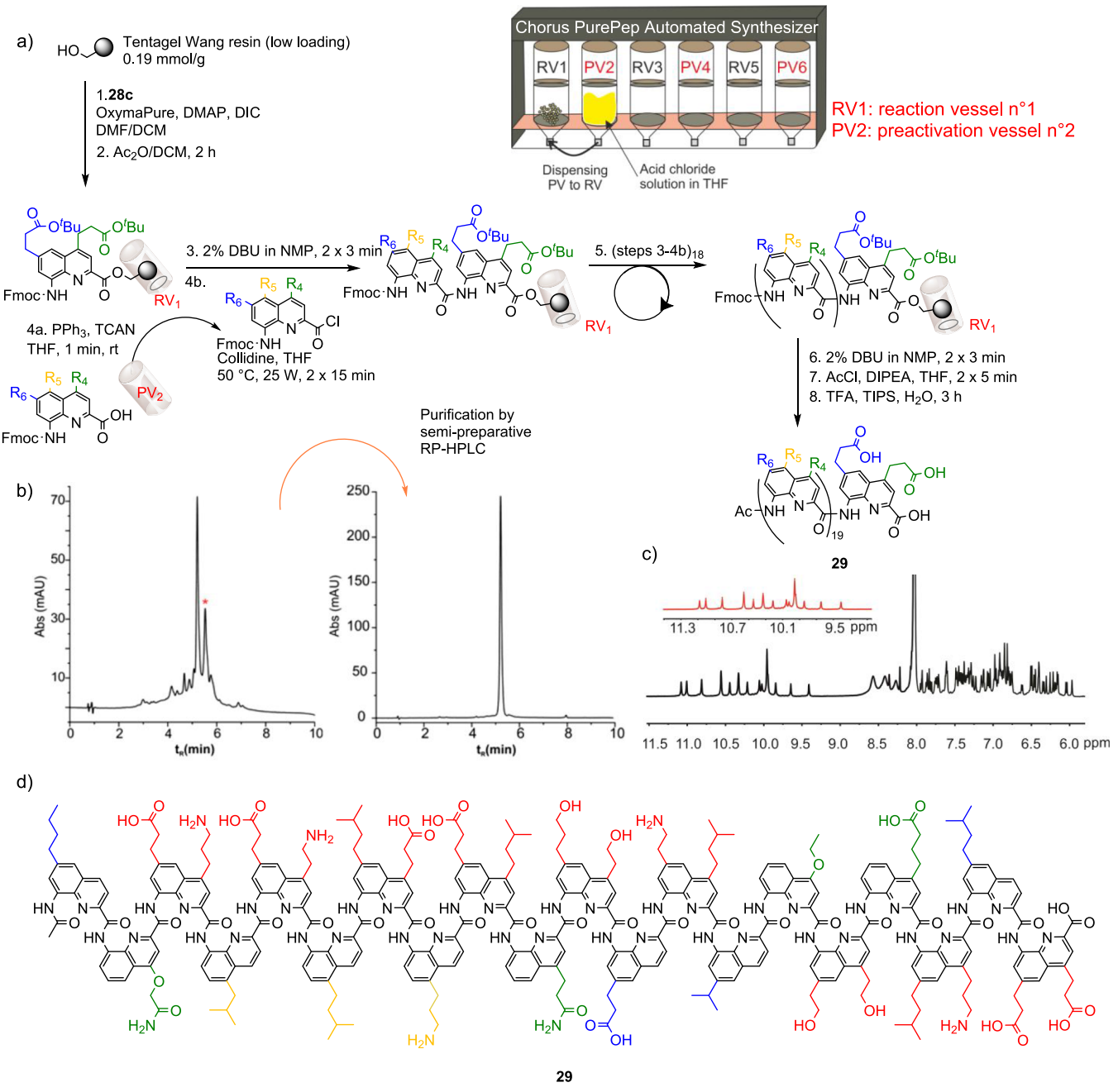

Figure 2. (a) SPFS (solid-phase foldamer synthesis) protocol recently developed, allowing the automation of the deprotection/coupling cycle for each of the 19 different aromatic monomers. The Chorus Purepep synthesizer is depicted to emphasize the *in situ* preactivation step (4a), which is performed in an independent preactivation vessel for 1 min before dispensing the acid chloride solution in the reaction vessel containing the resin swollen in THF with collidine. (b) RP-HPLC chromatograms of the 20mer (**29**), 75 mg as crude and after purification via RP-HPLC (linear gradient from 20% B to 80% B in 15 min, A: H_2O + 0.1% TFA and B: CH_3CN + 0.1% TFA, C8 column. (c) ^1H NMR of purified 20mer (**29**) in DMF-d_7 (500 MHz) at 0.5 mM at 298 K in black, NH amide region highlighted in red. (d) 20mer foldamer representation with position 4 monosubstituted monomer with green side chains, position 5-monosubstituted with golden side chains, position 6 monosubstituted with blue side chains, and position 4,6 disubstituted with red side chains. DIPEA: *N,N*-diisopropylethylamine, DIC: diisopropylcarbodiimide.

folding also include the anisochronicity of the diastereotopic CH_2 proton resonances of the side chains in ^1H NMR spectra. Methods to assign these spectra and to demonstrate helical conformations in solution have been reported.[65] An energy-minimized model of **29** is shown in Figure 3 along with a helix-wheel representation of the position of the side chains. Both highlight the side chain density that can be achieved by combining 4-, 5-, and 6-substituted monomers along with 4,6-disubstituted units.

CONCLUSION

Oligoamides built from natural amino acids and their close analogs form an indispensable part of today's research toolbox in medicinal chemistry and chemical biology. This is largely due to the fact that their building blocks are accessible in a large variety and that their construction has been automated, allowing for the efficient preparation of diverse libraries. While aromatic foldamers showed great promise as peptide mimetics due to their inherent self-organization potential and the possibility to

https://doi.org/10.1021/acs.joc.4c02900
J. Org. Chem. 2025, 90, 3043−3052

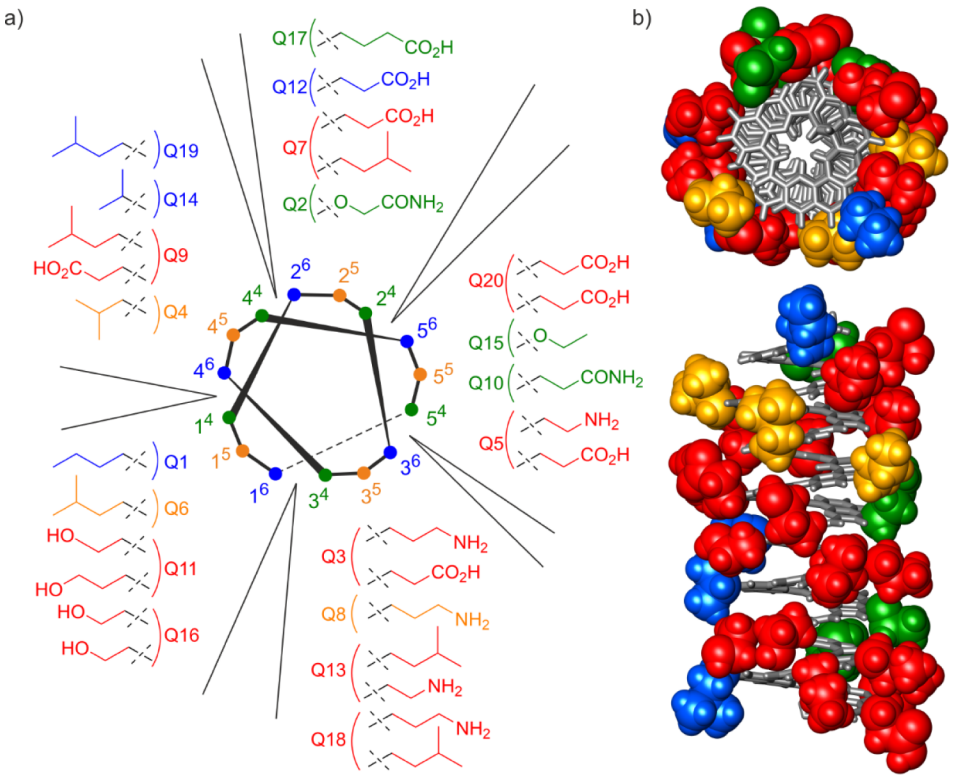

Figure 3. (a) Helix wheel representation of sequence **29**. The numbers around the wheel indicate the five first monomers, and their exponent refers to the possible position of their side chains. Monomers with one side chain in position 4, 5, or 6 are colored in green, gold, or blue, respectively. Monomers with side chains in positions 4 and 6 are shown in red. In all of the cases, the side chain shown on top is in position 4 and that below is in position 6. (b) Top view and side view of an energy minimized (MMFFs force field in Maestro)[66] model of sequence **29**. The main chain is shown in a gray tube representation. The side chains are shown in space-filling representation and are color-coded as in (a).

achieve high pharmacophore density on their surface, their widespread use was hampered both by limited access to building blocks and tedious process of oligomer assembly.

Using some easily accessible common building blocks, we developed a modular synthetic approach that allows for the introduction of various side chains into any of the desired positions on the aromatic foldamer core. The approach was validated through the preparation of 4-, 5-, and 6- mono-substituted, as well as 4,6-disubstituted foldamer building blocks. The prepared compounds carry a collection of side chains—apolar, polar, aromatic, acidic, and basic in nature—that mimic the natural diversity of amino acids. Finally, we demonstrated that a combination of the diverse monomer building blocks with the recently developed automated foldamer synthesis removes the technical barrier from the widespread use of this compound class. A 20mer consisting of 20 different building blocks and carrying a structural design that might be relevant for biological applications (i.e., similar pharmacophores being concentrated on the same part of the foldamer surface) was prepared in less than a day and was isolated in good overall yield and high purity. Expansion of this work to address biological problems is in progress in our laboratories.

■ ASSOCIATED CONTENT

Data Availability Statement

The data underlying this study are available in the published article and its Supporting Information.

Supporting Information

The Supporting Information is available free of charge at https://pubs.acs.org/doi/10.1021/acs.joc.4c02900.

Experimental details, materials, methods, and characterization data, including copies of NMR spectra (PDF)

■ AUTHOR INFORMATION

Corresponding Authors

Ivan Huc − *Ludwig-Maximilians-Universität, München 81377, Germany*; orcid.org/0000-0001-7036-9696; Email: ivan.huc@cup.lmu.de

András Kotschy − *Servier Research Institute of Medicinal Chemistry, Budapest 1031, Hungary*; orcid.org/0000-0002-7675-3864; Email: andras.kotschy@servier.com

Authors

Márton Zwillinger − *Servier Research Institute of Medicinal Chemistry, Budapest 1031, Hungary*

Petra Sőregi − *Servier Research Institute of Medicinal Chemistry, Budapest 1031, Hungary; Hevesy György PhD School of Chemistry, Eötvös Loránd University, Budapest 1117, Hungary*

Florian Sanchez − *Ludwig-Maximilians-Universität, München 81377, Germany*

Céline Douat − *Ludwig-Maximilians-Universität, München 81377, Germany*; orcid.org/0000-0003-2678-1047

Márton Csékei − *Servier Research Institute of Medicinal Chemistry, Budapest 1031, Hungary*; orcid.org/0000-0002-5781-1096

Complete contact information is available at: https://pubs.acs.org/10.1021/acs.joc.4c02900

https://doi.org/10.1021/acs.joc.4c02900
J. Org. Chem. 2025, 90, 3043−3052

Author Contributions

[#]M.Z., P.S., and F.S. contributed equally. The manuscript was written with contributions from all authors.

Notes

The authors declare no competing financial interest.

■ ACKNOWLEDGMENTS

Project C1016600 has been implemented with the support provided by the Ministry of Culture and Innovation of Hungary from the National Research, Development and Innovation Fund, financed under the KDP-2020 funding scheme (P.S.).

■ REFERENCES

(1) Seedorf, T.; Kirschning, A.; Solga, D. Natural and Synthetic Oligoarylamides: Privileged Structures for Medical Applications. *Chem. -Eur. J.* **2021**, *27* (26), 7321−7339.
(2) Zeelen, J.; van Straaten, M.; Verdi, J.; Hempelmann, A.; Hashemi, H.; Perez, K.; Jeffrey, P. D.; Hälg, S.; Wiedemar, N.; Mäser, P.; Papavasiliou, F. N.; Stebbins, C. E. Structure of Trypanosome Coat Protein VSGsur and Function in Suramin Resistance. *Nat. Microbiol.* **2021**, *6* (3), 392−400.
(3) Salvador, G. H. M.; Dreyer, T. R.; Gomes, A. A. S.; Cavalcante, W. L. G.; Dos Santos, J. I.; Gandin, C. A.; De Oliveira Neto, M.; Gallacci, M.; Fontes, M. R. M. Structural and Functional Characterization of Suramin-Bound MjTX-I from Bothrops Moojeni Suggests a Particular Myotoxic Mechanism. *Sci. Rep.* **2018**, *8*, 10317.
(4) Jiao, L.; Ouyang, S.; Liang, M.; Niu, F.; Shaw, N.; Wu, W.; Ding, W.; Jin, C.; Peng, Y.; Zhu, Y.; Zhang, F.; Wang, T.; Li, C.; Zuo, X.; Luan, C.-H.; Li, D.; Liu, Z.-J. Structure of Severe Fever with Thrombocytopenia Syndrome Virus Nucleocapsid Protein in Complex with Suramin Reveals Therapeutic Potential. *J. Virol.* **2013**, *87* (12), 6829−6839.
(5) Murakami, M. T.; Arruda, E. Z.; Melo, P. A.; Martinez, A. B.; Calil-Eliás, S.; Tomaz, M. A.; Lomonte, B.; Gutiérrez, J. M.; Arni, R. K. Inhibition of Myotoxic Activity of Bothrops Asper Myotoxin II by the Anti-Trypanosomal Drug Suramin. *J. Mol. Biol.* **2005**, *350* (3), 416−426.
(6) Salvador, G. H. M.; Dreyer, T. R.; Cavalcante, W. L. G.; Matioli, F. F.; Dos Santos, J. I.; Velazquez-Campoy, A.; Gallacci, M.; Fontes, M. R. M. Structural and Functional Evidence for Membrane Docking and Disruption Sites on Phospholipase A2-like Proteins Revealed by Complexation with the Inhibitor Suramin. *Acta Crystallogr., Sect. D: Biol. Crystallogr.* **2015**, *71*, 2066−2078.
(7) Zhou, X.; Tan, T. -C.; Valiyaveettil, S.; Go, M. L.; Kini, R. M.; Velazquez-Campoy, A.; Sivaraman, J. Structural Characterization of Myotoxic Ecarpholin S from Echis Carinatus Venom. *Biophys. J.* **2008**, *95* (7), 3366−3380.
(8) Mastrangelo, E.; Pezzullo, M.; Tarantino, D.; Petazzi, R.; Germani, F.; Kramer, D.; Robel, I.; Rohayem, J.; Bolognesi, M.; Milani, M. Structure-Based Inhibition of Norovirus RNA-Dependent RNA Polymerases. *J. Mol. Biol.* **2012**, *419* (3−4), 198−210.
(9) Baumann, S.; Herrmann, J.; Raju, R.; Steinmetz, H.; Mohr, K. I.; Hüttel, S.; Harmrolfs, K.; Stadler, M.; Müller, R. Cystobactamids: Myxobacterial Topoisomerase Inhibitors Exhibiting Potent Antibacterial Activity. *Angew. Chem., Int. Ed.* **2014**, *53* (52), 14605−14609.
(10) Michalczyk, E.; Hommernick, K.; Behroz, I.; Kulike, M.; Pakosz-Stępień, Z.; Mazurek, L.; Seidel, M.; Kunert, M.; Santos, K.; von Moeller, H.; Loll, B.; Weston, J. B.; Mainz, A.; Heddle, J. G.; Süssmuth, R. D.; Ghilarov, D. Molecular Mechanism of Topoisomerase Poisoning by the Peptide Antibiotic Albicidin. *Nat. Catal.* **2023**, *6* (1), 52−67.
(11) Hashimi, S. M. Albicidin, a Potent DNA Gyrase Inhibitor with Clinical Potential. *J. Antibiot.* **2019**, *72* (11), 785−792.
(12) Baraldi, P. G.; Del Carmen Nûnez, M.; Espinosa, A.; Romagnoli, R. Distamycin A as Stem of DNA Minor Groove Alkylating Agents. *Curr. Top. Med. Chem.* **2004**, *4*, 231−239.
(13) Hiraku, Y.; Oikawa, S.; Kawanishi, S. Distamycin A, a Minor Groove Binder, Changes Enediyne-Induced DNA Cleavage Sites and Enhances Apoptosis. *Nucleic Acids Res.* **2002**, *2*, 95−96.
(14) Paul, A.; Guo, P.; Boykin, D. W.; Wilson, W. D. A New Generation of Minor-Groove-Binding—Heterocyclic Diamidines That Recognize G·C Base Pairs in an AT Sequence Context. *Molecules* **2019**, *24* (5), 946.
(15) Wang, C. C. C.; Ellervik, U.; Dervan, P. B. Expanding the Recognition of the Minor Groove of DNA by Incorporation of β-Alanine in Hairpin Polyamides. *Bioorg. Med. Chem.* **2001**, *9*, 653−657.
(16) Matsuda, H.; Fukuda, N.; Ueno, T.; Tahira, Y.; Ayame, H.; Zhang, W.; Bando, T.; Sugiyama, H.; Saito, S.; Matsumoto, K.; Mugishima, H.; Serie, K. Development of Gene Silencing Pyrrole-Imidazole Polyamide Targeting the TGF-B1 Promoter for Treatment of Progressive Renal Diseases. *J. Am. Soc. Nephrol.* **2006**, *17* (2), 422−432.
(17) Dey, D.; Ramakumar, S.; Conn, G. L. Targeted Redesign of Suramin Analogs for Novel Antimicrobial Lead Development. *J. Chem. Inf. Model.* **2021**, *61* (9), 4442−4454.
(18) Parveen, N.; Lin, Y. L.; Chou, R. H.; Sun, C. M.; Yu, C. Synthesis of Novel Suramin Analogs With Anti-Proliferative Activity via FGF1 and FGFRD2 Blockade. *Front. Chem.* **2022**, *9*, 764200.
(19) Paulson, C. N.; John, K.; Baxley, R. M.; Kurniawan, F.; Orellana, K.; Francis, R.; Sobeck, A.; Eichman, B. F.; Chazin, W. J.; Aihara, H.; Georg, G. I.; Hawkinson, J. E.; Bielinsky, A. K. The Anti-Parasitic Agent Suramin and Several of Its Analogues Are Inhibitors of the DNA Binding Protein Mcm10. *Open Biol.* **2019**, *9* (8), 1−10.
(20) Roe, W. E.; Warnock, T. M. C.; Knipe, P. C. A Spirocyclic Backbone Accesses New Conformational Space in an Extended, Dipole-Stabilized Foldamer. *Commun. Chem.* **2023**, *6* (71), 1−6.
(21) McCann, S.; Roe, W. E.; Agnew, H. E.; Knipe, P. C. Non-Covalent Interactions Enforce Conformation in Switchable and Water-Soluble Diketopiperazine-Pyridine Foldamers. *Angew. Chem., Int. Ed.* **2023**, *62* (35), 1−5.
(22) Yin, H.; Lee, G. I.; Park, H. S.; Payne, G. A.; Rodriguez, J. M.; Sebti, S. M.; Hamilton, A. D. Terphenyl-Based Helical Mimetics That Disrupt the P53/HDM2 Interaction. *Angew. Chem., Int. Ed.* **2005**, *44* (18), 2704−2707.
(23) Raghuraman, A.; Ko, E.; Perez, L. M.; Ioerger, T. R.; Burgess, K. Pyrrolinone-Pyrrolidine Oligomers as Universal Peptidomimetics. *J. Am. Chem. Soc.* **2011**, *133* (32), 12350−12353.
(24) Moon, H.; Lee, W. S.; Oh, M.; Lee, H.; Lee, J. H.; Im, W.; Lim, H. S. Design, Solid-Phase Synthesis, and Evaluation of a Phenyl-Piperazine-Triazine Scaffold as α-Helix Mimetics. *ACS Comb. Sci.* **2014**, *16* (12), 695−701.
(25) Bayly, A. R.; White, A. J. P.; Spivey, A. C. Design and Synthesis of a Prototype Scaffold for Five-Residue α-Helix Mimetics. *Eur. J. Org. Chem.* **2013**, *2013* (25), 5566−5569.
(26) Jung, K. Y.; Vanommeslaeghe, K.; Lanning, M. E.; Yap, J. L.; Gordon, C.; Wilder, P. T.; Mackerell, A. D.; Fletcher, S. Amphipathic α-Helix Mimetics Based on a 1,2-Diphenylacetylene Scaffold. *Org. Lett.* **2013**, *15* (13), 3234−3237.
(27) Tew, G. N.; Liu, D.; Chen, B.; Doerksen, R. J.; Kaplan, J.; Carroll, P. J.; Klein, M. L.; DeGrado, W. F. De Novo Design of Biomimetic Antimicrobial Polymers. *Proc. NatI. Acad. Sci.* **2002**, *99* (8), 5110−5114.
(28) Lopez, C. F.; Nielsen, S. O.; Srinivas, G.; DeGrado, W. F.; Klein, M. L. Probing Membrane Insertion Activity of Antimicrobial Polymers via Coarse-Grain Molecular Dynamics. *J. Chem. Theory Comput.* **2006**, *2* (3), 649−655.
(29) Plante, J. P.; Burnley, T.; Malkova, B.; Webb, M. E.; Warriner, S. L.; Edwards, T. A.; Wilson, A. J. Oligobenzamide Proteomimetic Inhibitors of the P53-HDM2 Protein-Protein Interaction. *Chem. Commun.* **2009**, No. 34, 5091−5093.
(30) Saraogi, I.; Hebda, J. A.; Becerril, J.; Estroff, L. A.; Miranker, A. D.; Hamilton, A. D. Synthetic α-Helix Mimetics as Agonists and Antagonists of Islet Amyloid Polypeptide Aggregation. *Angew. Chem., Int. Ed.* **2010**, *49* (4), 736−739.
(31) Flack, T.; Romain, C.; White, A. J. P.; Haycock, P. R.; Barnard, A. Design, Synthesis, and Conformational Analysis of Oligobenzanilides as Multifacial α-Helix Mimetics. *Org. Lett.* **2019**, *21* (12), 4433−4438.

https://doi.org/10.1021/acs.joc.4c02900
J. Org. Chem. 2025, 90, 3043−3052

(32) Dohoney, R. A.; Joseph, J. A.; Baysah, C.; Thomas, A. G.; Siwakoti, A.; Ball, T. D.; Kumar, S. "Common-Precursor" Protein Mimetic Approach to Rescue Aβ Aggregation-Mediated Alzheimer's Phenotypes. *ACS Chem. Biol.* **2023**, *18* (7), 1510−1522.
(33) Arrata, I.; Grison, C. M.; Coubrough, H. M.; Prabhakaran, P.; Little, M. A.; Tomlinson, D. C.; Webb, M. E.; Wilson, A. J. Control of Conformation in α-Helix Mimicking Aromatic Oligoamide Foldamers through Interactions between Adjacent Side-Chains. *Org. Biomol. Chem.* **2019**, *17* (15), 3861−3867.
(34) Burslem, G. M.; Kyle, H. F.; Breeze, A. L.; Edwards, T. A.; Nelson, A.; Warriner, S. L.; Wilson, A. J. Small-Molecule Proteomimetic Inhibitors of the HIF-1α-P300 Protein-Protein Interaction. *ChemBioChem* **2014**, *15* (8), 1083−1087.
(35) Kumar, S.; Hamilton, A. D. α-Helix Mimetics as Modulators of Aβ Self-Assembly. *J. Am. Chem. Soc.* **2017**, *139* (16), 5744−5755.
(36) Alex, J. M.; Corvaglia, V.; Hu, X.; Engilberge, S.; Huc, I.; Crowley, P. B. Crystal Structure of a Protein-Aromatic Foldamer Composite: Macromolecular Chiral Resolution. *Chem. Commun.* **2019**, *55* (74), 11087−11090.
(37) Reddy, P. S.; Langlois d'Estaintot, B.; Granier, T.; Mackereth, C. D.; Fischer, L.; Huc, I. Structure Elucidation of Helical Aromatic Foldamer−Protein Complexes with Large Contact Surface Areas. *Chem. -Eur. J.* **2019**, *25* (47), 11042−11047.
(38) Buratto, J.; Colombo, C.; Stupfel, M.; Dawson, S. J.; Dolain, C.; Langlois D'Estaintot, B.; Fischer, L.; Granier, T.; Laguerre, M.; Gallois, B.; Huc, I. Structure of a Complex Formed by a Protein and a Helical Aromatic Oligoamide Foldamer at 2.1 Å Resolution. *Angew. Chem., Int. Ed.* **2014**, *53* (3), 883−887.
(39) Kumar, S.; Birol, M.; Schlamadinger, D. E.; Wojcik, S. P.; Rhoades, E.; Miranker, A. D. Foldamer-Mediated Manipulation of a Pre-Amyloid Toxin. *Nat. Commun.* **2016**, *7*, 11412.
(40) Ahmed, J.; Fitch, T. C.; Donnelly, C. M.; Joseph, J. A.; Ball, T. D.; Bassil, M. M.; Son, A.; Zhang, C.; Ledreux, A.; Horowitz, S.; Qin, Y.; Paredes, D.; Kumar, S. Foldamers Reveal and Validate Therapeutic Targets Associated with Toxic α-Synuclein Self-Assembly. *Nat. Commun.* **2022**, *13*, 2273.
(41) Ziach, K.; Chollet, C.; Parissi, V.; Prabhakaran, P.; Marchivie, M.; Corvaglia, V.; Bose, P. P.; Laxmi-Reddy, K.; Godde, F.; Schmitter, J. M.; Chaignepain, S.; Pourquier, P.; Huc, I. Single Helically Folded Aromatic Oligoamides That Mimic the Charge Surface of Double-Stranded B-DNA. *Nat. Chem.* **2018**, *10* (5), 511−518.
(42) Corvaglia, V.; Carbajo, D.; Prabhakaran, P.; Ziach, K.; Mandal, P. K.; Santos, V. D.; Legeay, C.; Vogel, R.; Parissi, V.; Pourquier, P.; Huc, I. Carboxylate-Functionalized Foldamer Inhibitors of HIV-1 Integrase and Topoisomerase 1: Artificial Analogues of DNA Mimic Proteins. *Nucleic Acid Res.* **2019**, *47* (11), 5511−5521.
(43) Kleene, V.; Corvaglia, V.; Chacin, E.; Forne, I.; Konrad, D. B.; Khosravani, P.; Douat, C.; Kurat, C. F.; Huc, I.; Imhof, A. DNA Mimic Foldamers Affect Chromatin Composition and Disturb Cell Cycle Progression. *Nucleic Acid Res.* **2023**, *51* (18), 9629−9642.
(44) Corvaglia, V.; Wu, J.; Deepak, D.; Loos, M.; Huc, I. Enhancing the Features of DNA Mimic Foldamers for Structural Investigations. *Chem. -Eur. J.* **2024**, *30* (16), No. e202303650.
(45) Bindl, D.; Mandal, P. K.; Huc, I. Generalizing the Aromatic δ-Amino Acid Foldamer Helix. *Chem. -Eur. J.* **2022**, *28*, No. e202200538.
(46) Zheng, L.; Zheng, D.; Wang, Y.; Yu, C.; Zhang, K.; Jiang, H. Chiral Bisphosphine Ligands Based on Quinoline Oligoamide Foldamers: Application in Asymmetric Hydrogenation. *Org. Biomol. Chem.* **2019**, *17* (44), 9573−9577.
(47) Yang, L.; Ma, C.; Kauffmann, B.; Li, D.; Gan, Q. Absolute Handedness Control of Oligoamide Double Helices by Chiral Oxazolylaniline Induction. *Org. Biomol. Chem.* **2020**, *18* (34), 6643−6650.
(48) Dawson, S. J.; Mészáros, Á.; Peth, L.; Colombo, C.; Csékei, M.; Kotschy, A.; Huc, I. Controlling Helix Handedness in Water-Soluble Quinoline Oligoamide Foldamers. *Eur. J. Org. Chem.* **2014**, *2014* (20), 4265−4275.
(49) Liu, Z.; Hu, X.; Abramyan, A. M.; Mészáros; Csékei, M.; Kotschy, A.; Huc, I.; Pophristic, V. Computational Prediction and Rationalization, and Experimental Validation of Handedness Induction in Helical Aromatic Oligoamide Foldamers. *Chem. -Eur. J.* **2017**, *23* (15), 3605−3615.
(50) Bindl, D.; Heinemann, E.; Mandal, P. K.; Huc, I. Quantitative Helix Handedness Bias through a Single H vs. CH3 Stereochemical Differentiation. *Chem. Commun.* **2021**, *57* (46), 5662−5665.
(51) Zwillinger, M.; Reddy, P. S.; Wicher, B.; Mandal, P. K.; Csékei, M.; Fischer, L.; Kotschy, A.; Huc, I. Aromatic Foldamer Helices as α-Helix Extended Surface Mimetics. *Chem. -Eur. J.* **2020**, *26* (72), 17366−17370.
(52) Hu, X.; Dawson, S. J.; Mandal, P. K.; De Hatten, X.; Baptiste, B.; Huc, I. Optimizing Side Chains for Crystal Growth from Water: A Case Study of Aromatic Amide Foldamers. *Chem. Sci.* **2017**, *8* (5), 3741−3749.
(53) Jayatunga, M. K. P.; Thompson, S.; Hamilton, A. D. α-Helix Mimetics: Outwards and Upwards. *Bioorg. Med. Chem. Lett.* **2014**, *24* (3), 717−724.
(54) Lanning, M. E.; Fletcher, S. Multi-Facial, Non-Peptidic α-Helix Mimetics. *Biology* **2015**, *4* (3), 540−555.
(55) Qi, T.; Deschrijver, T.; Huc, I. Large-Scale and Chromatography-Free Synthesis of an Octameric Quinoline-Based Aromatic Amide Helical Foldamer. *Nat. Protoc.* **2013**, *8* (4), 693−708.
(56) Corvaglia, V.; Sanchez, F.; Menke, F. S.; Douat, C.; Huc, I. Optimization and Automation of Helical Aromatic Oligoamide Foldamer Solid-Phase Synthesis. *Chem. -Eur. J.* **2023**, *29* (36), No. e202300898.
(57) Elgaher, W. A. M.; Hamed, M. M.; Baumann, S.; Herrmann, J.; Siebenburger, L.; Krull, J.; Cirnski, K.; Kirschning, A.; Bronstrup, M.; Muller, R.; Hartmann, R. W. Cystobactamid 507: Concise Synthesis, Mode of Action, and Optimization toward More Potent Antibiotics. *Chem. -Eur. J.* **2020**, *26* (32), 7219−7225.
(58) Sőregi, P.; Zwillinger, M.; Vágó, L.; Csékei, M.; Kotschy, A. High Density Information Storage through Isotope Ratio Encoding. *Chem. Sci.* **2024**, *15*, 14938.
(59) Guzmán, F.; Aróstica, M.; Román, T.; Beltrán, D.; Gauna, A.; Albericio, F.; Cárdenas, C. Peptides, Solid-Phase Synthesis and Characterization: Tailor-Made Methodologies. *Electron. J. Biotechnol.* **2023**, *64*, 27−33.
(60) Dengler, S.; Mandal, P. K.; Allmendinger, L.; Douat, C.; Huc, I. Conformational Interplay in Hybrid Peptide-Helical Aromatic Foldamer Macrocycles. *Chem. Sci.* **2021**, *12* (33), 11004−11012.
(61) Baptiste, B.; Douat-Casassus, C.; Laxmi-Reddy, K.; Godde, F.; Huc, I. Solid Phase Synthesis of Aromatic Oligoamides: Application to Helical Water-Soluble Foldamers. *J. Org. Chem.* **2010**, *75* (21), 7175−7185.
(62) Deepak, D.; Wu, J.; Corvaglia, V.; Allmendinger, L.; Scheckenbach, M.; Tinnefeld, P.; Huc, I. DNA Mimic Foldamer Recognition of a Chromosomal Protein. *Angew. Chem., Int. Ed.* **2025**, No. e202422958.
(63) Lee, M. A.; Brown, J. S.; Loas, A.; Pentelute, B. L. Investigation of Commercially Available Resins for the Automated Flow Synthesis of Difficult or Long Peptide Sequences. *Pept. Sci.* **2024**, *116* (3), No. e24344.
(64) Wang, S.; Wicher, B.; Douat, C.; Maurizot, V.; Huc, I. Domain Swapping in Abiotic Foldamers. *Angew. Chem., Int. Ed.* **2024**, *63* (28), No. e202405091.
(65) Dolain, C.; Grélard, A.; Laguerre, M.; Jiang, H.; Maurizot, V.; Huc, I. Solution Structure of Quinoline- and Pyridine-Derived Oligoamide Foldamers. *Chem. -Eur. J.* **2005**, *11* (21), 6135−6144.
(66) Schrödinger, LLC. *Maestro*; Schrödinger, LLC: New York, NY, 2021.

https://doi.org/10.1021/acs.joc.4c02900
J. Org. Chem. 2025, 90, 3043−3052